



TITLE:

Analyzing Power and Continuous Energy Spectrum for Three Body : Breakup Reaction in the DD Collision at 60 MeV

AUTHOR(S):

Fukunaga, K.; Kakigi, S.; Ohsawa, T.; Okihara, A.; Sekioka, T.; Nakamura-Yokota, H.; Murayama, T.; Hayashi, T.

CITATION:

Fukunaga, K. ...[et al]. Analyzing Power and Continuous Energy Spectrum for Three Body : Breakup Reaction in the DD Collision at 60 MeV. Bulletin of the Institute for Chemical Research, Kyoto University 1989, 67(1): 1-6

ISSUE DATE:

1989-03-31

URL:

<http://hdl.handle.net/2433/77291>

RIGHT:

Analyzing Power and Continuous Energy Spectrum for Three Body Breakup Reaction in the DD Collision at 60 MeV

K. FUKUNAGA*, S. KAKIGI*, T. OHSAWA*, A. OKIHANA**, T. SEKIOKA***,
H. NAKAMURA-YOKOTA****, T. MURAYAMA***** and T. HAYASHI*****

Received January 23, 1989

Three body breakup reactions were studied by measuring analyzing powers and continuous energy spectra of particles emitted in the dd collision at 60 MeV. The angular distribution of analyzing powers and that of cross sections in the FSI region were compared with three body model calculations.

KEY WORDS: Nuclear reactions/ Three body model/ Multiple scattering/

1. INTRODUCTION

At intermediate energies, the four nucleon reaction such as the $^3\text{He}(p, \text{pd})p$ quasi free scattering (QFS) was studied experimentally¹⁾ and analyzed with a plane wave impulse approximation (PWIA) calculation with a multiple scattering correction. In the case of the dd collision, energy spectra of emitted charged particles for the $^2\text{H}(\text{d}, \text{d})\text{pn}$ and $^2\text{H}(\text{d}, \text{p})^2\text{Hn}$ reactions were obtained²⁾ and analyzed with a four body theory assuming a first Born approximation and reasonable results were obtained in the breakup cross sections. In the dd breakup reaction, there are two types of reaction, one is a target deuteron breakup process and the other is a projectile deuteron breakup process. Furthermore an effect of the final state interactions (FSI) is expected at the highest energy region in the continuous energy spectrum. Thus it is interesting to see the effects of these reaction types and the FSI in the continuous energy spectrum and analyzing power distribution.

The purpose of the present experiment is to obtain experimental data of cross sections and analyzing powers for the $^2\text{H}(\vec{\text{d}}, \text{d})^1\text{Hn}$ inelastic scattering and $^2\text{H}(\vec{\text{d}}, \text{p})^2\text{Hn}$ breakup reaction. These data are analyzed with a three body theory.

2. EXPERIMENTAL PROCEDURE

A vector polarized deuteron beam from the AVF cyclotron of RCNP (Research Center for Nuclear Physics of Osaka University) was brought to a large scattering chamber. The beam energy was 59.8 MeV. The beam polarization was monitored by

* 福永清二, 柿木 茂, 大澤孝夫: Institute for Chemical Research, Kyoto University, Kyoto.

** 沖花 彰: Kyoto University of Education, Kyoto.

*** 関岡嗣久: Himeji Institute of Technology, Himeji.

**** 横田 轟: Faculty of Science, Tokyo Institute of Technology, Tokyo.

***** 村山利幸: Tokyo University of Mercantile Marine, Tokyo.

***** 林 俊治: Faculty of Science, Kyoto University, Kyoto.

a polarimeter consisting of two scintillation counters set at 47.5 degrees symmetrically to the beam direction and a carbon target at the focusing point of the beam course. The average polarization was 54.2% through the data taking time of the experiment. A gas chamber which was full of deuterium gas at 3 atm. had three windows of 10 μm Havar foil and was set at the center of the scattering chamber. A counter telescope was used to detect charged particles and was set on a turn table. The telescope consisted of a ΔE detector of 150 μm Si SSD and an E detector of 25 mm NaI(Tl) scintillator. A double slit system made of lead was used.

Energy scales were checked with energies of scattered deuterons for the $^2\text{H}(d, d)^2\text{H}$ elastic scattering and also checked with energies of recoiled protons for the $^1\text{H}(d, p)^2\text{H}$ elastic scattering.

3. THEORETICAL CALCULATION FOR THE BREAKUP REACTION

The breakup amplitude in the FSI region can be written with a AGS equation assuming the second Born approximation³⁾ as,

$$\begin{aligned} \langle p_r q_f | U_{0\alpha} G_0 | \alpha q_i \rangle = & (1 - \delta_{\beta\alpha}) \langle p_\beta | t_\beta | (C_{qq}^{\beta\alpha} q_\beta - q_i) / C_{qp}^{\beta\alpha} \rangle \Phi((q_\beta - C_{qq}^{\beta\alpha} q_i) / C_{qp}^{\beta\alpha}) / |C_{qp}^{\beta\alpha}|^3 \\ & - 2\pi^2 \kappa_\alpha \Sigma \eta_{\beta\delta\alpha} \langle p_\beta | t_\beta | (C_{qq}^{\delta\alpha} q_i - C_{qq}^{\delta\beta} q_\beta) / C_{qp}^{\delta\alpha} \rangle \\ & * \langle (C_{qq}^{\delta\alpha} C_{qq}^{\delta\beta} q_i - q_\beta) / C_{qp}^{\delta\beta} | t_\delta | C_{pq}^{\delta\alpha} q_i \rangle \Phi(0) / |C_{qp}^{\delta\alpha}|^3, \end{aligned} \quad (1)$$

$$\eta_{\beta\delta\alpha} = \zeta_{\beta\delta\alpha} [1 - \zeta_{\beta\delta\alpha} (\kappa_\alpha + i p_\beta) / \kappa_\alpha], \quad (2)$$

$$\zeta_{\beta\delta\alpha} = |C_{qp}^{\delta\beta} / C_{qp}^{\delta\alpha}| \kappa_\alpha / [\kappa_\alpha^2 + (C_{qq}^{\delta\alpha} q_i - C_{qq}^{\delta\beta} q_\beta)^2 / C_{qp}^{\delta\alpha 2}]^{1/2}.$$

Notation in Eq. (1) and (2) are the same as those in Ref. 3. The breakup cross section is proportional to the absolute square of Eq. (1). In the case of inelastic scattering, the interacting pair β in the final channel is the same as the interacting pair α in the initial channel. When the breakup process is caused through only one interaction of pair δ , the cross section is proportional to the two body T matrix of pair δ and it can be written as,

$$\partial\sigma/\partial\omega_\alpha \partial E_\alpha \propto (E_\alpha \cdot E_{\text{RCM}})^{1/2} |\eta_{\alpha\delta\alpha}|^2 (\partial\sigma/\partial\omega)_\delta. \quad (3)$$

The first term $(E_\alpha \cdot E_{\text{RCM}})^{1/2}$ comes from the phase space factor of three body breakup reaction. To calculate the analyzing power for the breakup reaction, Eq. (1) must be written in a spin state dependent form. But in the case of neglecting the spin state dependence of the final state interaction, the analyzing power of the breakup reaction can be reduced from the analyzing power for the two body scattering of pair δ .

4. RESULTS AND DISCUSSIONS

Fig. 1 shows the continuous energy spectra and spin analyzing power distributions for the $^2\text{H}(\vec{d}, d)\text{pn}$ inelastic scattering. At forward angles, the energy spectrum has a

Analyzing Power and Continuous Energy Spectrum

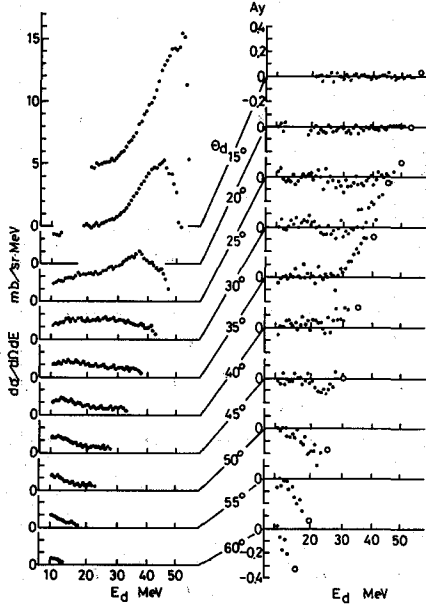


Fig. 1. Angular dependence of continuous energy spectra and that of analyzing power distributions for the $^2\text{H}(\text{d}, \text{d})\text{pn}$ breakup reaction at 59.7 MeV. Circles in the analyzing power distribution show the data for the elastic scattering.

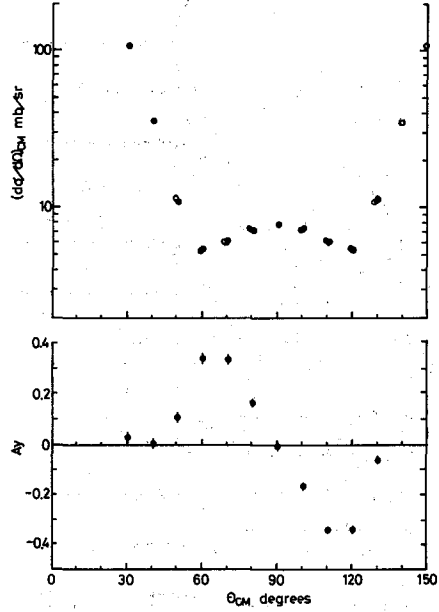


Fig. 2. Angular dependences of differential cross section and analyzing power for the $^2\text{H}(\bar{\text{d}}, \text{d})^2\text{H}$ elastic scattering at 59.7 MeV. In the upper half, the point at θ is plotted again at $\pi - \theta$ with circle.

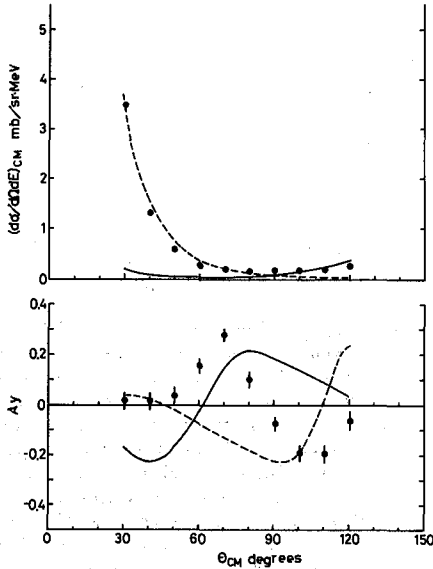


Fig. 3. Angular dependences of differential cross section and analyzing power for the $^2\text{H}(\bar{\text{d}}, \text{d})\text{pn}$ inelastic scattering at 59.7 MeV. The curve in the upper half show the cross sections calculated using Eq. (3). The curves in the lower half show the calculated angular dependences of analyzing power. The solid and dashed curves correspond to the projectile breakup and target breakup processes, respectively.

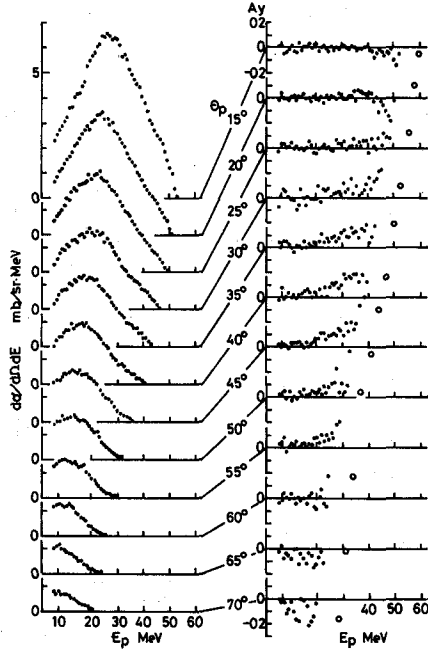


Fig. 4. Angular dependence of continuous energy spectra and that of analyzing power distributions for the $^2\text{H}(\bar{d}, p)^2\text{Hn}$ breakup reaction at 59.7 MeV. Circles in the analyzing power distributions show the data for the $^2\text{H}(\bar{d}, p)^3\text{H}$ two body reaction.

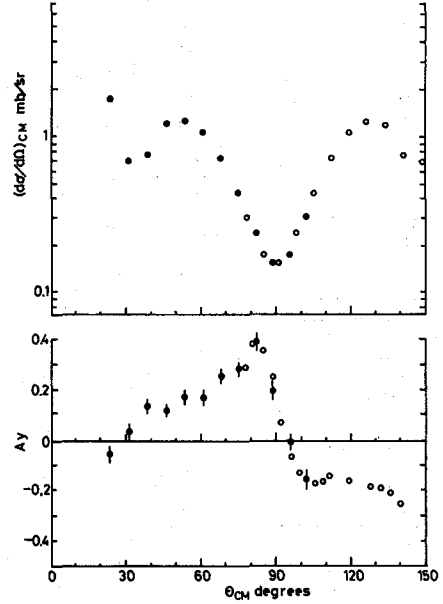


Fig. 5. Angular dependences of differential cross section and analyzing power for the $^2\text{H}(\bar{d}, p)^3\text{H}$ reaction at 59.7 MeV. In the upper half, the point at θ is plotted again at $\pi-\theta$ with circle. Circles in the lower half show the data for the $^2\text{H}(\bar{d}, t)p$ reaction at 56 MeV by Nisimura et al⁹.

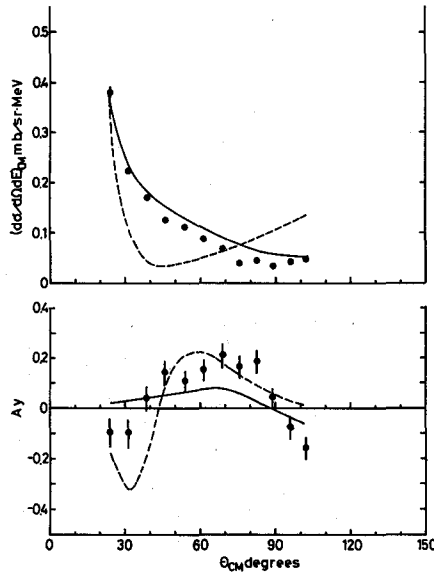


Fig. 6. Angular dependences of differential cross section and analyzing power for the $^2\text{H}(\bar{d}, p)^2\text{Hn}$ breakup reaction. The solid and dashed curves show the calculated cross sections for the projectile breakup and the target breakup processes, respectively. The solid and the dashed curves of analyzing powers are calculated from those for the dp scattering at 56 MeV⁴⁾ and for the pd scattering with polarized protons at 30 MeV^{6,7)}, respectively.

sharp edge and a large bump in the highest energy region. Nonzero analyzing powers are seen in this high energy region, and the angular dependence of analyzing power is similar to that of the elastic scattering, which are shown with open circles in the figure.

Fig. 2 shows angular dependence of the cross section and that of the analyzing power for the ${}^2\text{H}(\vec{d}, d){}^2\text{H}$ elastic scattering and Fig. 3 shows angular dependence of the cross section and that of the analyzing power for the ${}^2\text{H}(\vec{d}, d)\text{pn}$ inelastic scattering in the energy region from the breakup threshold to the excitation energy of 2.7 MeV. The angular dependence of the inelastic cross section shows a forward peak and a rather smooth distribution in comparison with that for the elastic scattering. The solid curve in the upper half of Fig. 3 corresponds to the projectile breakup calculation and it can not reproduce the experimental data. The dashed curve was calculated assuming the target breakup process and normalized to the maximum cross section at the most forward angle. The forward peak is reproduced with the target breakup calculation. The analyzing power of the dashed curve, which was reduced from the data of the ${}^1\text{H}(\vec{d}, d){}^1\text{H}$ elastic scattering at 56 MeV⁴⁾, shows an opposite sign to the experimental data for the inelastic scattering in the angular range smaller than 90°.

Fig. 4 shows the continuous energy spectra and spin analyzing power distributions of protons for the ${}^2\text{H}(\vec{d}, p){}^2\text{Hn}$ reaction. Large bumps are seen near the middle of the energy spectrum at forward angles. The energy of the maximum yield is several MeV lower than the optimum QFS energy which is estimated from the energy of recoiled protons for the ${}^1\text{H}(d, p){}^2\text{H}$ elastic scattering. The cross section shows a large forward peak and this forward peak was reproduced by the single NN scattering in a four body model calculation²⁾. The analyzing power shows almost flat zero distribution. Therefore these large bumps seem to be explained by the single NN scattering. Nonzero analyzing powers are seen in the highest energy region. The angular dependence of the analyzing power at the highest energy is also similar to that for the ${}^2\text{H}(\vec{d}, p){}^3\text{H}$ two body reaction as shown with open circles in the figure.

Fig. 5 shows the angular dependences of the differential cross sections and the analyzing power for the ${}^2\text{H}(\vec{d}, p){}^3\text{H}$ two body reaction and the angular distribution shows a diffraction like pattern. The data of analyzing power are smoothly connect with the triton observed data for the ${}^2\text{H}(\vec{d}, t){}^1\text{H}$ reaction at 56 MeV⁵⁾.

Fig. 6 shows the angular dependence of the cross section and that of the analyzing power for the ${}^2\text{H}(\vec{d}, p){}^2\text{Hn}$ breakup reaction in the energy region from the threshold to the excitation energy of 2.6 MeV. The cross section of three body break up process has no diffraction like pattern. The curves in the figure show the calculated cross sections. The curves are normalized to the maximum cross section in the experimental data. The large forward peak is reproduced by the projectile break up calculation (the solid curve) or the target breakup calculation (the dashed curve) as shown in the figure. The curve for the target breakup process has the minimum cross section at 40° which is corresponding to the minimum cross section for the dp scattering at 120°.

The experimental data of analyzing power has the same sign with the analyzing power for the ${}^2\text{H}(\vec{d}, p){}^3\text{H}$ two body process. The solid curve of analyzing power corresponding to the projectile breakup process was reduced from the data for the dp scattering with polarized protons at 30 MeV^{6,7)} and shows the same sign but the rather small in

comparison with the experimental data. The dashed curve corresponding to the target breakup process is reduced from the data with the vector polarized deuterons at 56 MeV³). In the case of target deuteron breakup process, the proton in the target is recoiled out and detected. Therefore the proton angle θ is corresponding to the angle $\pi-\theta$ for the dp scattering center of mass system and the sign of analyzing power is opposite. Both analyzing power calculations show the same sign as the experimental data in the range from 40° to 90° as shown in Fig. 6. Eq. (1) is obtained assuming a three body model. Hence, both processes can not be treated with at the same time but the experimental data means that both processes seem to contribute in this breakup reaction.

In conclusion, the FSI is an important process of three body breakup reaction in the dd collision and the FSI process is explained using the three body model of the multiple scattering theory. The analyzing power of the inelastic scattering can not be explained by the three body model calculation and more complete analyses are expected to reproduce the experimental data.

This experiment was done at RCNP for the program No. of 25A11, and the data were analyzed at the computer center of Institute for Chemical Research of Kyoto University.

REFERENCES

- 1) S. Kakigi, K. Fukunaga, T. Ohsawa, A. Okihana, T. Sekioka, H. Nakamura-Yokota, S. Tanaka and S. Kato, *Nucl. Phys.* **A473**, 31 (1987).
- 2) K. Fukunaga, T. Ohsawa, S. Kakigi, A. Okihana, S. Tanaka, T. Sekioka and H. Nakamura-Yokota, *Nucl. Phys.* **A390**, 19 (1982).
- 3) K. Fukunaga, S. Kakigi, T. Ohsawa, A. Okihana and T. Sekioka, *Jour. Phys. Soc. Japan* **56**, 2357 (1987).
- 4) K. Hatanaka, N. Matsuoka, H. Sakai, T. Saito, K. Hosono, Y. Koike, M. Kodo, K. Imai, H. Shimizu, T. Ichihara, K. Nishimura and A. Okihana, *Nucl. Phys.* **A426**, 77 (1984).
- 5) K. Nishimura, K. Imai, T. Matsusue, H. Shimizu, R. Takashima, K. Hatanaka, T. Saito and A. Okihana, Annual Report of RCNP, p. 32, 1979.
- 6) A. R. Johnston, W. R. Gibson, J. H. P. C. Megraw, R. J. Griffiths and R. M. Eisberg, *Phys. Lett.* **19**, 289 (1965).
- 7) S. J. Hall, A. R. Johnston and R. J. Griffiths, *Phys. Lett.* **14**, 212 (1965).